

DEPARTMENT OF THE NAVY

HYDROMECHANICS

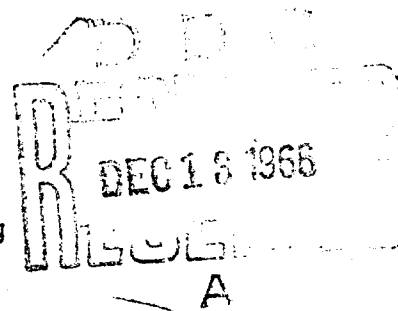
AERODYNAMICS

STRUCTURAL  
MECHANICSAPPLIED  
MATHEMATICSACOUSTICS AND  
VIBRATION

CLEARING HOUSE FOR FEDERAL SCIENTIFIC AND TECHNICAL INFORMATION		SLAMMING OF RIGID WEDGE-SHAPED BODIES WITH VARIOUS DEADRISE ANGLES	
Hardcopy	\$3.00	Microfiche	\$1.65
pp		39	
ARCHIVE COPY		code 1	

by

Sheng-Lun Chuang



Distribution of this document is unlimited.

STRUCTURAL MECHANICS LABORATORY  
RESEARCH AND DEVELOPMENT REPORT

October 1966

Report 2268

DAVID TAYLOR MODEL BASIN  
WASHINGTON, D. C. 20007

SLAMMING OF RIGID WEDGE-SHAPED BODIES  
WITH VARIOUS DEADRISE ANGLES

by

Sheng-Lun Chuang

Distribution of this document is unlimited.

October 1966

Report 2268  
S-R011 01 01  
Task 0401

## TABLE OF CONTENTS

	Page
ABSTRACT .....	1
ADMINISTRATIVE INFORMATION .....	1
INTRODUCTION .....	1
THEORETICAL BACKGROUND .....	2
DESCRIPTION OF MODELS AND TESTS .....	6
INSTRUMENTATION .....	7
PRESENTATION AND DISCUSSION OF TEST RESULTS .....	8
Detection of Trapped Air during Flat-Bottom Slamming.....	8
Effect of Deadrise Angle on Trapped Air .....	11
Effect of Deadrise Angle on Slamming Pressure .....	11
CONCLUSIONS AND SUMMARY .....	14
ACKNOWLEDGMENTS.....	14
REFERENCES .....	30

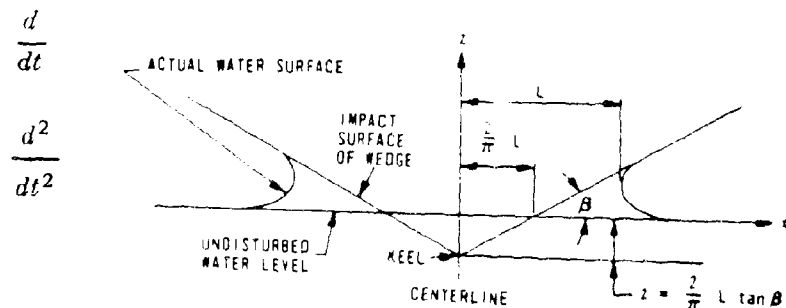
## LIST OF FIGURES

Figure 1 - Sketches of Rigid Flat-Bottom Model .....	15
Figure 2 - Sketches of Rigid Wedge-Shaped Models .....	16
Figure 3 - Drop-Test Facility .....	17
Figure 4 - Block Diagram of Recording System .....	18
Figure 5 - Diagram for Electronic Detection of Trapped Air .....	18
Figure 6 - Simplified Circuit Diagram of Trapped Air Detector .....	18
Figure 7 - Typical Record Showing Time Relationship between Occurrence of Maximum Impact Pressure and Occur- rence of Water Contact with Impact Surface of Rigid Flat-Bottom Body.....	19
Figure 8 - Underwater Photos Taken during 6-Inch Drop Tests of Rigid Wedge-Shaped Models with Various Deadrise Angles .....	20

	Page
Figure 9 – Samples of Records Taken during 6-Inch Drop Tests of Rigid Wedge-Shaped Models with Various Deadrise Angles .....	21
Figure 10 – Experimental Results of Maximum Impact Pressure Due to Rigid Wedge Slamming .....	23
Figure 11 – Maximum Impact Pressure Due to Rigid Wedge Slamming versus Various Drop Heights .....	26
Figure 12 – Maximum Impact Pressure Due to Rigid Wedge Slamming versus Various Deadrise Angles .....	28

## NOTATION

$c$	Speed of sound in fluid
$c_{\text{air}}$	Speed of sound in air
$i$	Current
$L$	Half wetted breadth of wedge measured horizontally, = $\pi/2$ of half breadth of wedge at undisturbed water level
$m_{zz}$	Added mass of fluid
$M_0$	Mass of falling body
$p$	Impact pressure in general
$P$	Total impact pressure in general
$R$	Resistance
$t$	Time in general
$T$	Period in general
$T_1$	Half period or duration of first positive pulse, = $T/2$
$V$	Voltage in general
$V$	Velocity in general
$V_0$	Impact velocity
$x, y$	Horizontal coordinates in $x, y, z$ coordinate system
$z$	Vertical coordinate in $x, y, z$ coordinate system
$z_0$	Vertical position at instant of impact
$\beta$	Deadrise angle, radian
$\rho$ or $\rho_{\text{fluid}}$	Mass density of fluid



## ABSTRACT

An experimental investigation of rigid body slamming was performed at the David Taylor Model Basin by dropping one flat-bottom steel model and five wedge-shaped steel models with small deadrise angles (from 1 to 15 deg) from various elevated positions above a calm water surface. Recording instrumentation was capable of picking up and recording frequencies from 0 to 200 kc, which covered the frequency range of the hydrodynamic as well as the acoustic pressures that might act on the model. From the test results, a set of charts is provided to predict the maximum impact pressures due to slamming of rigid wedge-shaped bodies.

## ADMINISTRATIVE INFORMATION

The experimental investigation of rigid wedge-shaped body slamming is being carried out as part of the plate-impact studies under the In-House Independent Research Program. This work is funded by Subproject S-R011 01 01, Task 0401.

## INTRODUCTION

In recent years, ship speed has become one of the important factors among competitors in private industry as well as in the navy in ship operations. The desire to increase the ship operational speed is obvious. When a ship is trying to maintain this increased speed during a heavy weather season, it is inevitable to experience the impact force of the wave at the bow. This type of impact force may easily damage the local ship-hull structure or cause the entire ship to vibrate for some time. The impact of any portion of a moving ship upon the surface wave is known to mariners by the term "slamming." Ship response due to slamming may be classified into three categories, namely, localized response, transitions, and overall response.

During and immediately after slamming, there is a period of localized response when the hull-plate panels will respond immediately, because of direct contact with the slamming load. Since keel, floors, and nearby frame structures function as supports to the hull plating, they also react without delay.

Following the initial period is one of transition when the stress wave is travelling at the speed of sound through the local hull structure, but the entire ship hull is not yet aware of the slamming load.

Finally, there follows a period of overall response. If the excited force, i.e., the slamming load, has produced sufficient momentum, the hull may vibrate transversely, longitudinally, torsionally, or in any combination of these, depending upon what portion or locality of the ship hull has been attacked by the slamming load. The transverse hull vibration is sometimes referred to as whipping.

Slamming damage of local ship-hull structure has been a puzzling problem to ship researchers as well as to ship designers. In view of this, it was decided to perform some basic experiments to determine the mechanics of local slamming phenomenon before getting into the complicated problem of structural damage due to slamming.

From previous fundamental studies,<sup>1, 2</sup> evidence has been found that the air trapped between the falling flat-bottom body and the water surface has a great effect on the magnitude of peak-impact pressure. The objective of present study is to determine the effect of various deadrise angles of the impact body on the trapped air and the impact-pressure time history. The deadrise angle is defined as the angle between the impact surface of falling body and the horizontal.

This report presents the work done in connection with rigid wedge-shaped body slamming and some of the conclusions resulting from the experimental work. It indicates that further tests are needed before the results can be considered conclusive. In addition, model constructions, test facility, and instrumentation are described; and the theoretical background concerning the rigid wedge-shaped body slamming is presented. Theoretical results are compared with the test results.

All tests discussed in this report were performed at the David Taylor Model Basin during the Fiscal Year 1966.

## THEORETICAL BACKGROUND

When a rigid body penetrates the water surface, the total hydrodynamic impact pressure  $P$  acting upon the impact surface may be obtained by<sup>3</sup>

$$P = -M_0 \ddot{z}$$

For the free falling body, the change in momentum is zero, or

$$(M_0 + m_{zz}) V - M_0 V_0 = 0$$

---

<sup>1</sup>References are listed on page 30.

At the instant of impact,

$$t_0 = 0, z_0 = 0, \text{ and } \dot{z}_0 = V_0$$

Thus,

$$V = \dot{z} = \frac{M_0 V_0}{M_0 + m_{zz}}$$

and

$$\dot{V} = \ddot{z} = - \frac{M_0 V_0 \dot{m}_{zz}}{(M_0 + m_{zz})^2}$$

This gives

$$P = -M_0 \ddot{z} = \frac{M_0^2 V_0 \dot{m}_{zz}}{(M_0 + m_{zz})^2} = \frac{V_0 \dot{m}_{zz}}{\left(1 + \frac{m_{zz}}{M_0}\right)^2} \quad [1]$$

Equation [1] shows that the added mass  $m_{zz}$  and the change of the added mass as a function of time  $\dot{m}_{zz}$  play a significant part in calculating the impact pressure. Various two-dimensional added-mass formulas have been derived for the case of the V-shaped wedge penetration, and a list of the few is shown as follows:<sup>4</sup>

$$\left. \begin{array}{ll} \text{von Kármán} & m_{zz} = \frac{\pi}{2} \rho \left(\frac{2L}{\pi}\right)^2 \\ \text{Wagner} & m_{zz} = \frac{\pi}{2} \rho L^2 \\ \text{Kreps} & m_{zz} = \frac{\pi}{2} \rho L^2 \left[1 - \frac{\beta}{\pi}\right] \\ \text{Wagner-Sydow} & m_{zz} = \frac{\pi}{2} \rho L^2 \left[\frac{\pi}{2\beta} - 1\right]^2 \left[\frac{2 \tan \beta}{\pi}\right]^2 \\ \text{Mayo} & m_{zz} = 0.82 \frac{\pi}{2} \rho L^2 \left[\frac{\pi}{2\beta} - 1\right]^2 \left[\frac{2 \tan \beta}{\pi}\right]^2 \\ \text{Monaghan} & m_{zz} = \frac{\pi}{2} \rho L^2 \left[1 - \frac{\beta}{\pi}\right]^3 \end{array} \right\} \quad [2]$$

If  $m_{zz} = \frac{\pi}{2} \rho L^2$  is used for Equation [1], it is easy to show that the total impact pressure  $P$  is

$$P = \frac{\pi}{2} \frac{\rho L V_0^2}{\left[1 + \frac{m_{zz}}{M_0}\right]^3 \beta}$$

Now that the total impact pressure is known, it is desirable to study the pressure distribution. The pressure distribution on the impact surface of a wedge penetrating through the water surface was derived by Wagner from the Bernoulli equation for unsteady potential flow.<sup>3</sup> This equation is

$$\frac{p}{\frac{1}{2} \rho V^2} = \frac{\pi}{\beta \sqrt{1 - \frac{x^2}{L^2}}} - \frac{\frac{x^2}{L^2}}{1 - \frac{x^2}{L^2}} + \frac{2\ddot{z}}{V^2} \sqrt{L^2 - x^2} \quad [3]$$

The maximum impact pressure  $p_{\max}$  is obtained by putting

$$\frac{dp}{dx} = 0$$

and assuming  $\ddot{z}$  to be small and therefore neglected. Thus

$$\frac{p_{\max}}{\frac{1}{2} \rho V^2} = 1 + \frac{\pi^2}{4\beta^2} \quad [4]$$

The maximum impact pressure occurs at

$$x = L \sqrt{1 - \frac{4\beta^2}{\pi^2}} \quad [5]$$

At keel,  $x = 0$ . From Equation [3], the impact pressure at the keel  $p_{\text{keel}}$  is

$$\frac{p_{\text{keel}}}{\frac{1}{2} \rho V^2} = \frac{\pi}{\beta} + \frac{2\ddot{z}}{V^2} L \quad [6]$$

If  $\ddot{z}$  is neglected,

$$\frac{p_{\text{keel}}}{\frac{1}{2} \rho V^2} = \frac{\pi}{\beta} \quad [7]$$

However, as derived by von Kármán,<sup>5</sup> the maximum impact pressure at keel at the moment of contact with water surface is,

$$\frac{p_{\text{keel}}}{\frac{1}{2} \rho V_0^2} = \frac{\pi}{\tan \beta} \quad [8]$$

which is identical to Equation [7] if  $\beta$  is small.

For the flat-bottom slamming, the deadrise angle  $\beta$  is zero. This means that the impact pressure  $p$  is infinitely large if Equation [3], [7], or [8] is applied. Therefore, as  $\beta$  approaches zero, Equations [3], [7], and [8] have no practical value.

An experimental investigation of rigid flat-bottom body slamming was performed at the Model Basin.<sup>1, 2</sup> It was observed that

1. The major reason for the maximum impact pressure of flat-bottom slamming being much lower than expected ( $\rho c V_0$  as per von Kármán<sup>5</sup>) is due to the existence of air trapped between the falling body and the water surface.

2. The effects produced by the compressible layer of air between the falling body and the water are as follows:

a. The rise time of the impact-pressure pulse is increased because of the cushioning effect of the compressible air.

b. Some of the air has to be pushed into the surface layer of water because the air cannot escape completely. This greatly reduces the value of  $\rho c$  because the surface layer becomes a nonhomogenous air-water mixture.

From the experimental observation and theoretical reasoning, the impact pressure for rigid flat-bottom body slamming was given by

$$p(t) = 2 p_{\text{max}} e^{-1.4 \frac{t}{T_1}} \sin \pi \frac{t}{T_1} \quad [9]$$

with

$$p_{\max} = \frac{1}{32(144)} \left[ \frac{1.4 + \pi^2}{e^{-1.4} + 1} \right] \rho_{\text{fluid}} c_{\text{air}} V_0 \quad [10]$$

$$T_1 = 4L c_{\text{air}} \quad [11]$$

where  $(1/144)$  is the factor to convert  $p_{\max}$  from psf units into psi units; since  $\rho_{\text{fluid}}$  is in lb-sec<sup>2</sup>/ft<sup>4</sup>,  $c_{\text{air}}$  is in fps, and  $V_0$  is in fps. Using  $\rho_{\text{fluid}} = 1.94$  lb-sec<sup>2</sup>/ft<sup>4</sup> for fresh water and  $c_{\text{air}} = 1125$  fps, Equation [10] reduces to

$$p_{\max} = 4.5 V_0 \quad [12]$$

## DESCRIPTION OF MODELS AND TESTS

Six models were tested in the present study. They were one rigid flat-bottom model and five rigid wedge-shaped models.

The rigid flat-bottom model is shown in Figure 1. It consisted of a 1 1/2- by 20- by 26 1/2-in. steel plate with welded 1/2- by 3-in. steel flat-bar stiffeners. The plate and the stiffeners were welded to a steel box. Thus, for drop heights of 7 1/2 in. and lower, the model may be considered as a rigid flat-bottom body. To assure the flatness of the test plate on the impact side, a three-quarter-inch plate was used for fabrication. After welding, the test plate was machined to a thickness of a little more than one-half inch. The combined weight of the steel box and the flat-plate model was 212 lb, and the total drop weight for the test was 255 lb. This total weight included the guided sliding beam and other necessary attachments.

The rigid wedge-shaped models are shown in Figure 2. They were essentially similar to the rigid flat-bottom model, except for the shorter edge of the test plate of each model, which was cut into two equal widths and then welded together to form a V-shaped wedge. The deadrise angles of the five models were 1, 3, 6, 10, and 15 deg, respectively. The method of fabrication of these models was essentially similar to that for the flat-bottom model. The combined weight of each steel box and the wedged-plate model ranged from 208 to 211 lb, but the total drop weight for each test was 255 lb.

The tests were conducted in the facility designed and built by the DTMB Hydromechanics Laboratory; see Figure 3. This facility is a large rectangular tank, 25 by 15 ft, filled with water to a depth of 8.5 ft. To ensure two-dimensional flow conditions, two vertical walls, made of steel plates, were constructed to span the length of the tank and to extend from 18 in. above the water surface to the full tank depth. The two parallel walls are rigidly connected

to the tank floor and sides and are separated by a distance equal to the model length of 26 1/2 in. plus a small amount of clearance. The parallel walls have open ends to permit free flow of the surface wave around the tank during the drop test.

The support and guide systems for the drop test consisted of a steel frame and a guided aluminum box beam; see Figure 3. The model was attached to the beam by two aluminum brackets, with rubber strips fitted between the brackets and the model to absorb the unwanted vibration caused by the drop test. The desired drop height was obtained by proper positioning of the sliding beam, which was guided so that maximum rotation of the model in any direction was limited to one-quarter degree during the drop.

The releasing mechanism consisted of a solenoid attached to the top member of the frame by an adjustable steel rod. The solenoid was equipped with a hook from which to hang the sliding beam. When the solenoid was activated, the hook was instantaneously released, and the beam and the model fell freely.

The drop heights, which are defined as the distance between the keel and the water surface, ranged from 3 to 7 1/2 in. at 1 1/2-in. increments. Pressures, accelerations, and two selected positions of the moving model were recorded. In addition, 16 mm high-speed movies, both underwater and surface, were taken to study water flow, piled-up water, and trapped air during and after the impact. The speed of the movie varied up to about 5000 frames per sec. Sufficient time was allowed for the camera to pick up speed before a drop was initiated.

## INSTRUMENTATION

The instrumentation system used for the experimental investigation consisted essentially of quartz-crystal transducers, charge amplifiers, a dual-beam oscilloscope, and a high-speed streak camera; see the block diagram shown in Figure 4. The charge amplifiers were the Kistler Model-568. These picked up a 200-kc signal without noticeable error. The oscilloscope was a Tektronix Type-551, with a frequency range from zero to  $25(10)^6$  cps. By means of the chop technique, four traces were displayed on the screen instead of two. The streak camera was a General Radio Type-651-A, with speeds up to 1000 ips, and it was fitted with suitable optics to view the screen of the oscilloscope. Also in view of the camera were two neon bulbs which served as "event markers." By means of beaded chain, one event marker flashed when the model had fallen 1 in. from the rest position. The other event marker flashed when the model had fallen to within 1 in. of the water surface. From these two event marks on the film, the velocity of the falling body could be checked.

The pressure gages were of Kistler Model-603 quartz-crystal, having a natural frequency of 200 kc and able to record a rise time of 1  $\mu$ sec. The validity of the pressure measurements of the complete recording system was tested electronically and mechanically, and was also

calibrated by an underwater explosion.<sup>1</sup> The results indicated that the entire recording system had the ability to pick up and record the high-frequency acoustic pressure, if it existed during the impact of the falling body with the water surface.

Piezoelectric accelerometers, Endevco Model-2225, were used to measure model acceleration near the center of the model. With a natural frequency of 80-ke, the gage was considered adequate for the drop test.

## PRESENTATION AND DISCUSSION OF TEST RESULTS

During the Fiscal Year 1965, a series of drop tests of a rigid flat-bottom model (0-deg deadrise angle) was conducted at the Model Basin to determine the origin of slamming pressure.<sup>1</sup> Based upon the observations of the trapped-air phenomenon, a theory for rigid flat-bottom slamming was developed. As outlined briefly in the section of theoretical background, the theory predicts the impact pressure upon the impact surface of a falling body during the occurrence of flat-bottom slamming. One of the assumptions was used in developing this theory that the first positive pulse of the impact pressure occurred during the split second when the air was trapped between the falling body and the water surface. Nevertheless, no evidence was available to determine whether the measured impact pressure was generated by the compression of the trapped air or by the actual contact of the falling body on the water surface.

Immediately after considering the trapped-air phenomenon, the effect of the deadrise angle of the ship bottom on the trapped air was questioned. Thus this series of tests was planned and performed to answer that question.

The shape of the wave formation during slamming of a wedge-shaped body was obtained from the underwater and surface high-speed movies. Owing to geometrical discontinuity at the edge of the box, the water was forced out tangentially to the impact surface of the wedge-shaped body and then curved upward to form a void space between the vertical wall of the box and the waterjet. The void space closed up, and the water struck the side wall of the box as the immersion velocity of the box was gradually reduced. This secondary slamming phenomenon was very much the same as presented in Reference 1 for the flat-bottom slamming, and therefore, that presentation is omitted in this report.

## DETECTION OF TRAPPED AIR DURING FLAT-BOTTOM SLAMMING

The electronic detection of trapped air was performed for the rigid flat-bottom model only. The trapped-air detecting equipment was not used for the other models largely because of limitations in time schedule. The method of detection is described in the following paragraphs.

As shown in Figure 5, the two probes are attached to and insulated from the impact surface of the flat-bottom model. If both of the probes are touched by a mass of water, the resistance across the two probes will be about 3000 ohms, depending on the distance between these probes. If the water does not connect two probes together, even though two probes are independently wet, the resistance across the points *B* and *E* will be practically infinite.

To demonstrate how the circuitry serves the purpose of trapped air detection, Figure 6, which is a simplified representation of the circuit shown in Figure 5, will be used for explanations. Let  $R_1$  represent the resistance across two probes which are the points *B* and *E* in the diagram. Use  $i_1$  as the current flowing through *B* and *E*.  $R_2$  is a 30-k resistor,  $V_{in}$  is the input voltage, and  $V_{out}$  is the output voltage.

For the Circuit Loop-1,

$$V_{in} = i_1(R_2 + R_1)$$

or

$$i_1 R_1 = \frac{V_{in}}{1 + \frac{R_2}{R_1}}$$

But from the Circuit Loop-2,

$$V_{out} = i_1 R_1$$

Thus,

$$V_{out} = \frac{V_{in}}{1 + \frac{R_2}{R_1}} \quad [13]$$

If the water does not touch both probes together

$$R_1 \rightarrow \infty$$

Then by Equation [13],

$$V_{out} = V_{in}$$

If a mass of water touches both probes,

$$R_i \approx 3k$$

Then by Equation [13],

$$V_{out} = \frac{V_{in}}{1 + \frac{30}{3}} = \frac{1}{11} V_{in}$$

In other words, at the instant a mass of water is in contact with the impact surface of the falling body, the voltage output signal will be reduced to one-eleventh of the input voltage. However, if the two probes are splashed wet by the water but are still separated by an air gap, the resistance across *B* and *E* is still large, and the change of the output signal will be relatively small.

Figure 7 shows a typical record providing evidences of the time relationship between the occurrence of the first positive pulse of the impact pressure and the occurrence of water actually in contact with the impact surface of the rigid flat-bottom body. As demonstrated in the figure, the trace with a 10-kc carrier signal is used to indicate whether or not a mass of water is actually in contact with the impact surface of the flat-bottom model. The large 10-kc signal indicates the existence of a layer of air trapped between the flat-bottom model and the water surface. The 10-kc signal with very small magnitude means that at that moment the water is actually in contact with the impact surface of the flat-bottom model.

The other trace of the record shown in Figure 7 is the time-history curve of the impact pressure measured at the center of the flat-bottom model. The curve provides the specific time when the maximum impact pressure occurs. For this particular record, the drop height was 6.5 in. The maximum impact pressure was 27 psi, which supported the flat-bottom impact theory very well. The maximum pressure occurred about 13 msec before the water came in contact with the impact surface of the flat-bottom body. In other words, only after completion of the first positive pulse of the impact pressure did the trapped air appear to have partly escaped and to have partly been pushed into the water surface layer.

From the observations and the analyzed data of the trapped-air detection tests, it is reasonable to conclude that, during the water surface impact, the first positive pulse of the impact pressure occurs when the air is momentarily trapped between the falling rigid flat-bottom body and the water surface.

## EFFECT OF DEADRISE ANGLE ON TRAPPED AIR

In response to the question on the effect of deadrise angle to the trapped air, a series of tests was planned and conducted by dropping five rigid wedge-shaped models with low-deadrise angles of 1, 3, 6, 10, and 15 deg, respectively. These models were described earlier. The trapped-air phenomenon was investigated by the underwater slow-motion camera and by the pressure measurements. All the movies were taken at a drop height of 6 in., and the pressure measurements were taken at drop heights of 3, 4.5, 6, and 7.5 in.

Figure 8 shows the underwater photographs taken during the drop test of the wedge-shaped models. The underwater photograph of the flat-bottom model is included for comparison. As it can be seen from the pictures, only the flat-bottom and the 1-deg models trap a considerable amount of air. For the models having deadrise angles of 3-deg and higher, most of the air escapes at the instant of impact. During the impact, the higher the deadrise angle the clearer the impact surface observed. However, this could be affected to some extent by the angle of the light source to the impact surface of the model.

Since 3 deg is not much deadrise and since the air is trapped for such a short duration, the trapped-air phenomenon is highly unstable with respect to time and the angle of impact. Thus the test results are sufficient to make a general conclusion that, during the impact, most of the air is pushed away by the wedge-shaped model with 3 deg or greater deadrise angle before its keel pierces through the water surface.

Evidence of the effect of the deadrise angle to the impact pressure is brought up in the subsection that follows.

## EFFECT OF DEADRISE ANGLE ON SLAMMING PRESSURE

In the section about theoretical background, the maximum impact pressures of the wedge are given by

1. Away from the keel (Wagner):

$$p_{\max} = \frac{1}{2} \rho V^2 \left[ 1 + \frac{\pi^2}{4\beta^2} \right] \quad [4]$$

2. At the keel (Wagner and Von Kármán):

$$p_{\text{keel}} = \frac{1}{2} \rho V_0^2 \left( \frac{\pi}{\beta} \right) \quad [7]$$

The maximum impact pressure of the flat-bottom model is given by

$$p_{\max} = 4.5 V_0^2 \quad [12]$$

Equations [4] and [7] are applicable for the large value of the deadrise angle  $\beta$  because the cushioning effect of the air can be neglected. As the value of  $\beta$  becomes less, the effect of air cushioning on the maximum impact pressure is greater. For small values of  $\beta$ , there are no theoretical equations to predict the impact pressure. Therefore, the wedge-shaped models with low-deadrise angles were used to resolve some of the uncertainties in the region where the deadrise angle of the wedge-shaped body would be small (for instance,  $\beta \leq 15$  deg).

Samples of records are shown in Figure 9. As can be seen from the records, the impact-pressure histories at the keel are quite different from those away from the keel. The impact pressure at the keel begins with an impulse, short in duration (less than 0.05 msec), then it is followed by the so-called hydrodynamic pressure. The impulse pressure at the keel is not pronounced for the 1-deg model, since the impact pressure is affected by the trapped air cushioning; see Figure 9a. With the exception of the 1-deg model, the impact pressure away from the keel steps up quickly with a rise time of about 0.1 msec; then it dies out slowly. The impact pressure histories of the 1-deg model closely resemble those of the flat-bottom model except that there is a time delay for the pressure measured further away from the keel.

The pressure measurement at the keel deserves some discussion. Theoretically, even an infinitesimal force will produce infinite pressure, since the force is applied to a line which has no area, and the pressure is the force divided by the area. The pressure gage used to measure the keel pressure has a non-zero area one-quarter inch in diameter. Therefore, if a different size of gage is used, the results may not be the same, especially the impulse pressure at the keel. However, based on the test results, the maximum impact pressures at the keel and away from the keel are plotted in Figure 10.

From plots on log-log charts, such as shown in Figure 10, the pressure-velocity relationship (or pressure-drop height relationship) may be obtained by fitting a straight line to the test data, since Equations [4], [7], and [12] can be rewritten in a general form

$$p = C V^n$$

which is a straight line on a log-log chart. Based on the experimental results, a straight line was fitted on a log-log chart for each model. These lines are shown in Figures 10a to 10e. From these, the coefficients of the formulas are calculated and are given as follows:

1. Flat bottom:  
At keel:

$$p_{\text{keel}} = 4.5 V_0$$

Away from keel:

$$p_{\text{max}} = 4.5 V_0$$

2. 1-deg deadrise angle:  
At keel:

$$p_{\text{keel}} = 3.15 V_0^{1.4}$$

Away from keel:

$$p_{\text{max}} = 3.15 V^{1.4}$$

3. 3-deg deadrise angle:  
At keel:

$$p_{\text{keel}} = 1.04 V_0^{1.6}$$

Away from keel:

$$p_{\text{max}} = 4.11 V^{1.6}$$

4. 6-deg deadrise angle:  
At keel:

$$p_{\text{keel}} = \frac{1}{2} \rho V_0^2 \left( \frac{\pi}{\beta} \right) \left( \frac{1}{144} \right)$$

Away from keel:

$$p_{\text{max}} = 0.87 V^2$$

5. 10-deg deadrise angle:  
At keel:

$$p_{\text{keel}} = \frac{1}{2} \rho V_0^2 \left( \frac{\pi}{\beta} \right) \left( \frac{1}{144} \right)$$

Away from keel:

$$p_{\text{max}} = 0.42 V^2$$

6. 15-deg deadrise angle:  
At keel:

$$p_{\text{keel}} = \frac{1}{2} \rho V_0^2 \left( \frac{\pi}{\beta} \right) \left( \frac{1}{144} \right)$$

Away from keel:

$$p_{\text{max}} = 0.24 V^2$$

7. 18-deg and above deadrise angles:  
At keel:

$$p_{\text{keel}} = \frac{1}{2} \rho V_0^2 \left( \frac{\pi}{\beta} \right) \left( \frac{1}{144} \right)$$

Away from keel:

$$p_{\text{max}} = \frac{1}{2} \rho V^2 \left[ 1 + \frac{\pi^2}{4\beta^2} \right] \left( \frac{1}{144} \right)$$

[14]

where (1.144) in Equation [14] is the factor for converting the impact pressure  $p$  from psf units into psi units; and  $\rho$  is in lb-sec<sup>2</sup>/ft<sup>4</sup>,  $\beta$  is in radians, and  $V$  and  $V_c$  are in fps. In Equation [14],  $\rho = 1.94$  lb-sec<sup>2</sup>/ft<sup>4</sup> is used for fresh water. For the sea water slamming problem, a correction of  $(\rho_{\text{sea water}}/\rho_{\text{fresh water}})$  should be applied.

Figure 11 is plotted from Equation [14] and Figure 12 is a cross plot of Figure 11. These may be used to predict the maximum slamming pressure of the ship bottom with various deadrise angles. If the deadrise angle is greater than 45 deg, Equation [4] and [7] may be used. No formula or plot is formulated for the impulse pressure at keel. Since the keel impulse pressure lasts only about 0.05 msec, it is probably not felt by the ship bottom. From the practical point of view, the impulse pressure at the keel may be ignored in the design of a ship bottom.

## CONCLUSIONS AND SUMMARY

On the basis of the analyses of experimental results, the following conclusions are drawn:

1. During the slamming of the rigid flat-bottom body, the first positive pulse of the impact pressure occurs when the air is momentarily trapped between the falling body and the water surface.
2. Only the flat bottom and the 1-deg wedge trap considerable amounts of air at the instant of impact. Wedges with 3-deg or more deadrise angles do not trap much air.
3. The maximum slamming pressure of the ship bottom may be predicted from Figures 11 and 12. Nevertheless, further test with much wider ranges of drop height are needed before the results can be considered conclusive.

## ACKNOWLEDGMENTS

The author expresses thanks to Messrs. A.B. Stavovy and L.A. Becker who initiated this fundamental study and assigned it to the author. The instrumentation system was developed by Mr. G.W. Cook and his assistants, Messrs. D.T. Milne and H.G. Eberhardt. The motion picture photography, both underwater and above water, was performed by Mr. B.C. Ball. The author acknowledges their expert assistance and valuable suggestions.

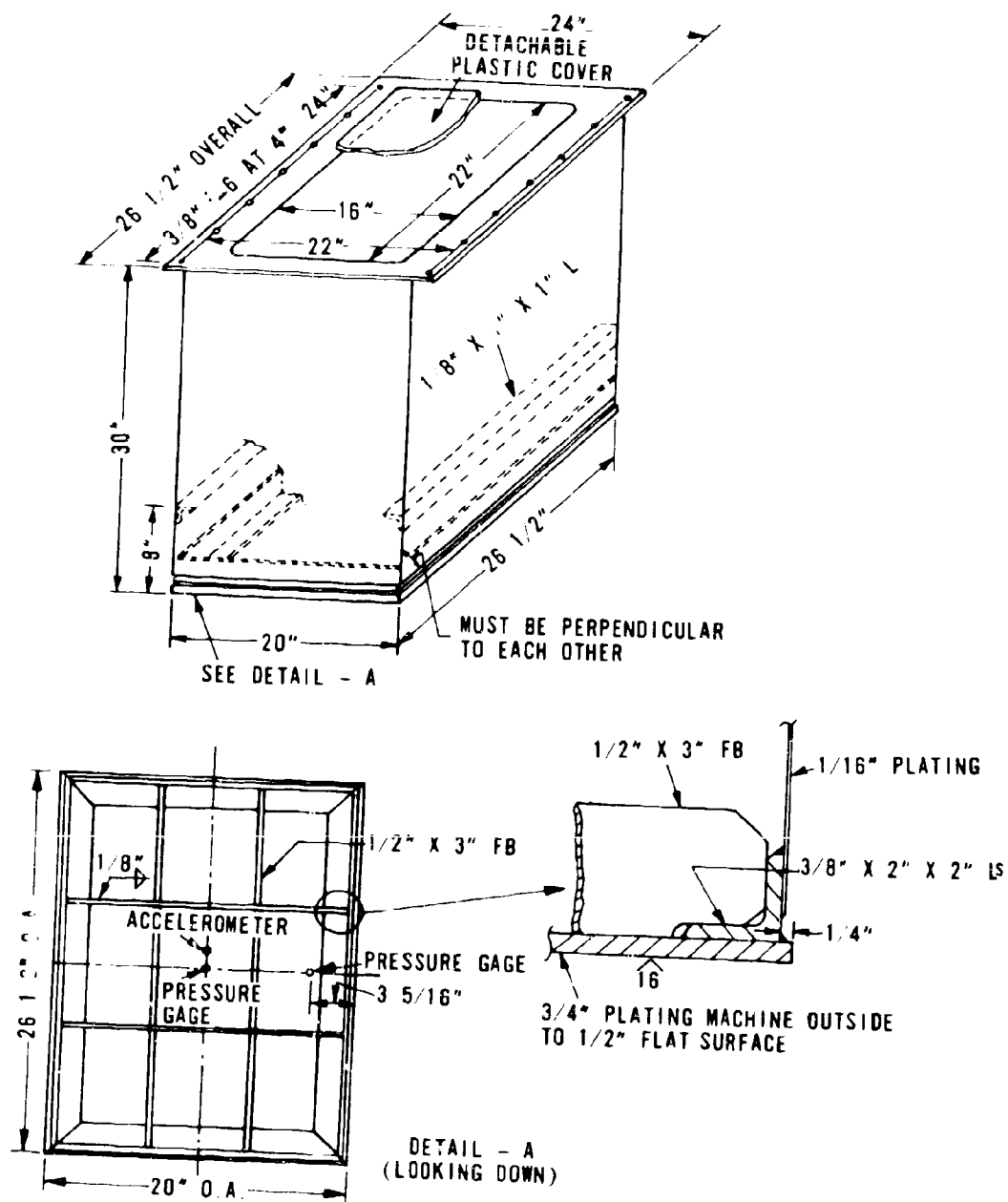
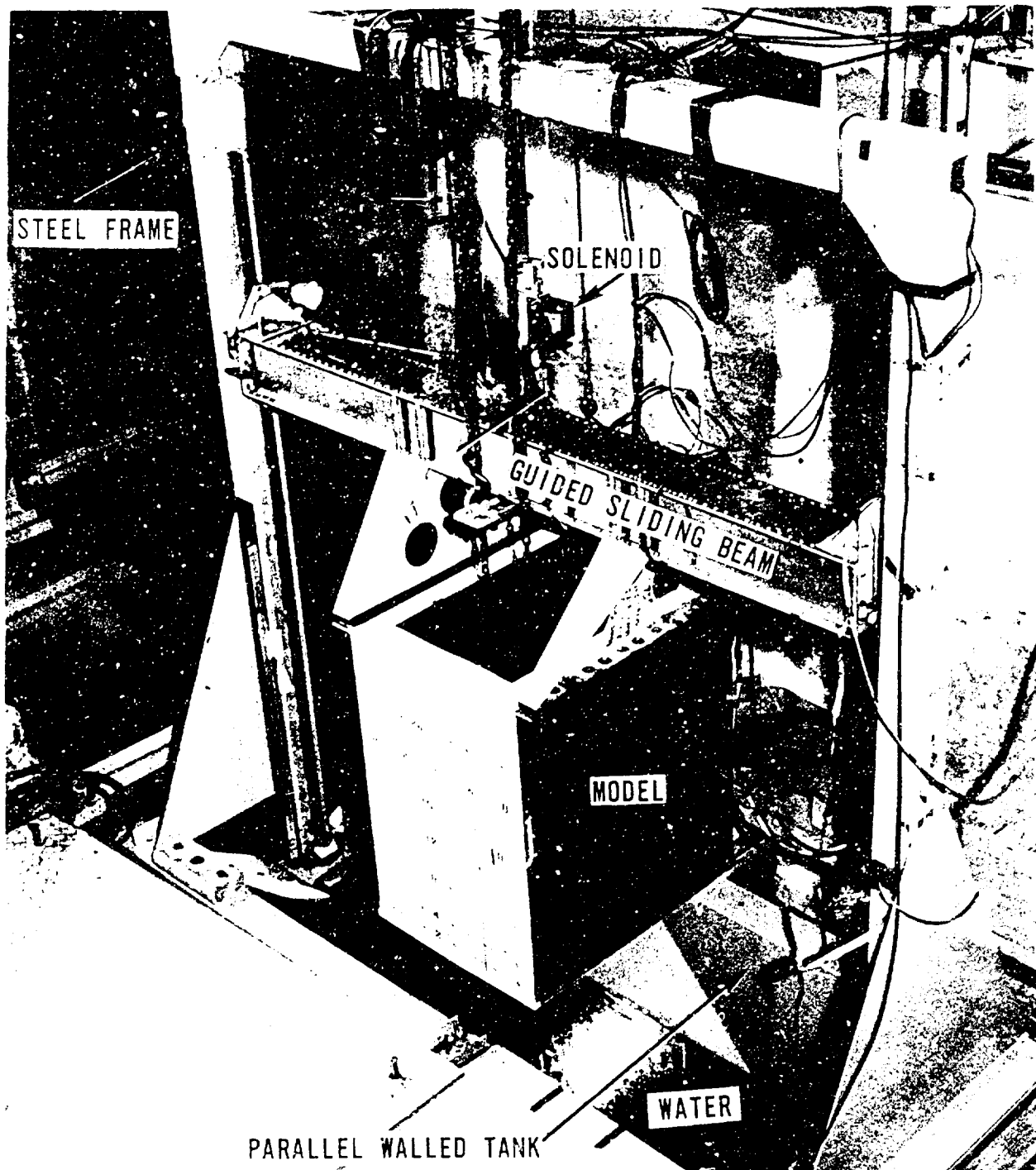


Figure 1 - Sketches of Rigid Flat-Bottom Model





PARALLEL WALLED TANK

Figure 3 — Drop-Test Facility

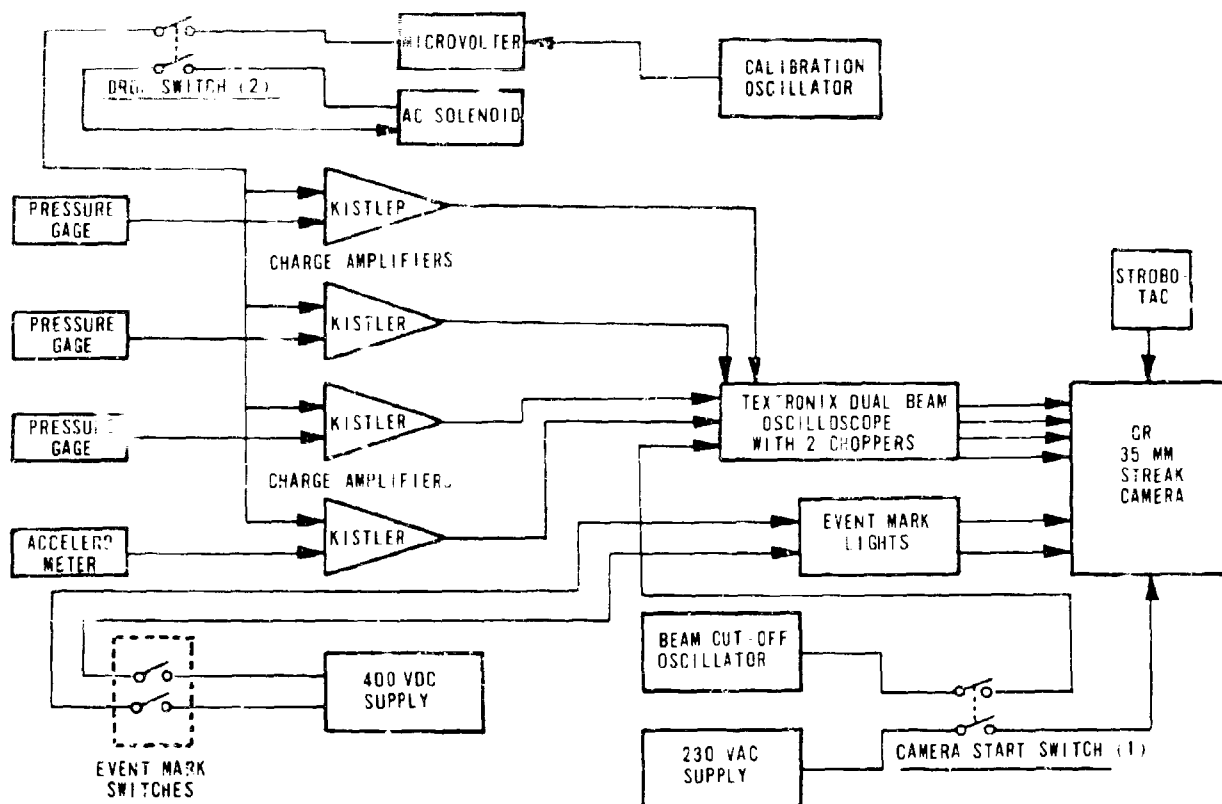


Figure 4 – Block Diagram of Recording System

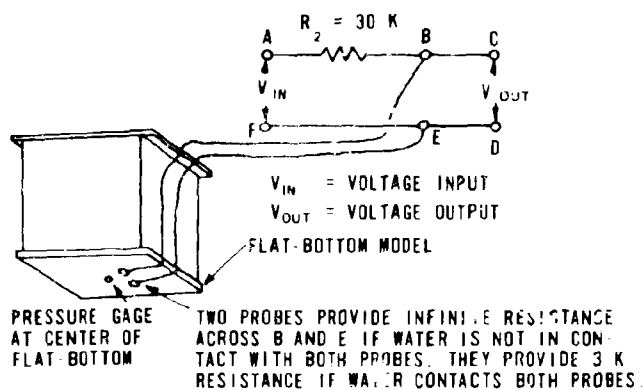


Figure 5 – Diagram for Electronic Detection of Trapped Air

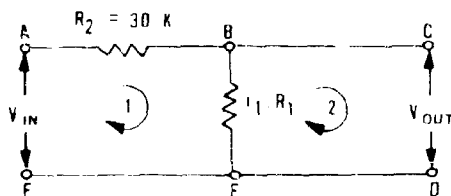


Figure 6 – Simplified Circuit Diagram of Trapped Air Detector

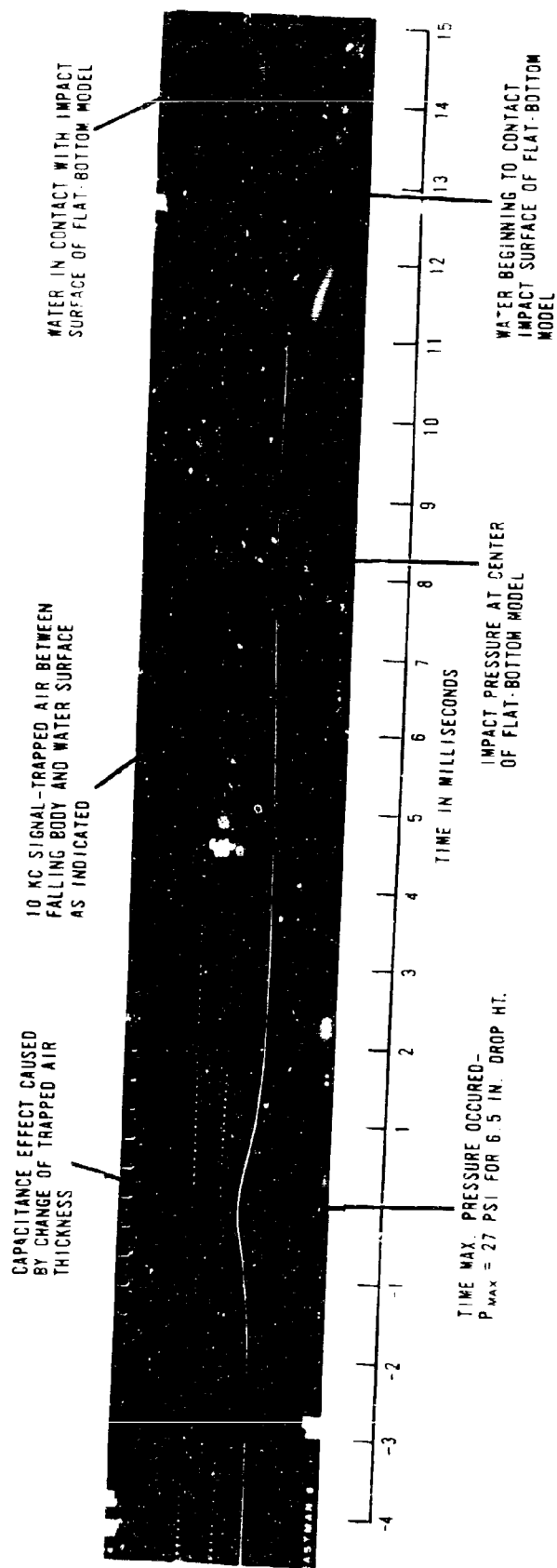
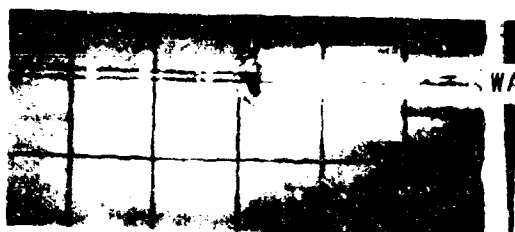
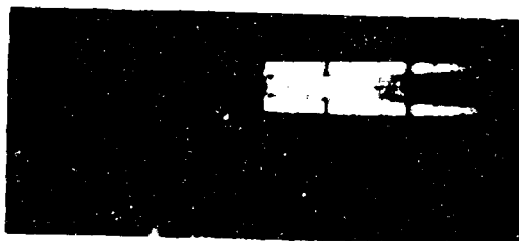
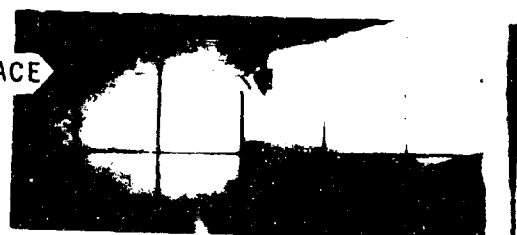


Figure 7 - Typical Record Showing Time Relationship between Occurrence of Maximum Impact Pressure and Occurrence of Water Contact with Impact Surface of Rigid Flat-Bottom Body



3 DEG DEADRISE MODEL



15 DEG DEADRISE MODEL

Figure 8 — Underwater Photos Taken during 6-Inch Drop Tests of Rigid Wedge-Shaped Models with Various Deadrise Angles

Figure 9 – Samples of Records Taken during 6-Inch Drop Tests of Rigid Wedge-Shaped Models with Various Deadrise Angles

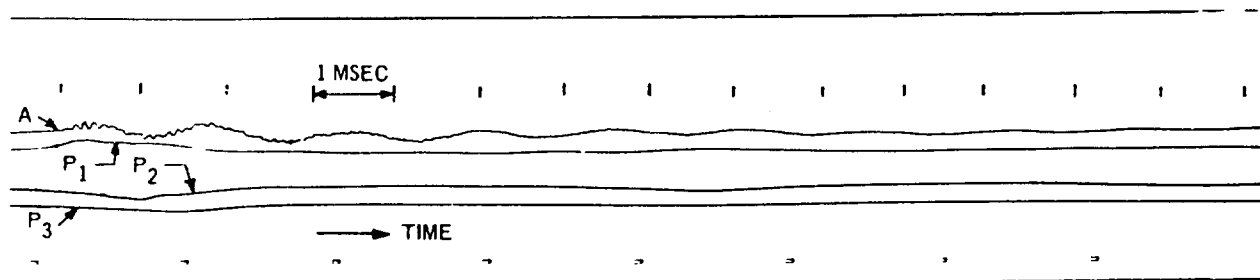


Figure 9a – 1-Degree Deadrise Model

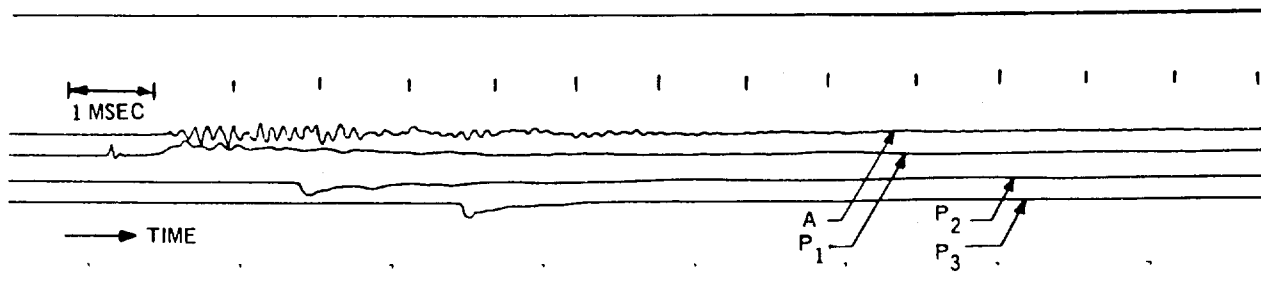


Figure 9b – 3-Degree Deadrise Model

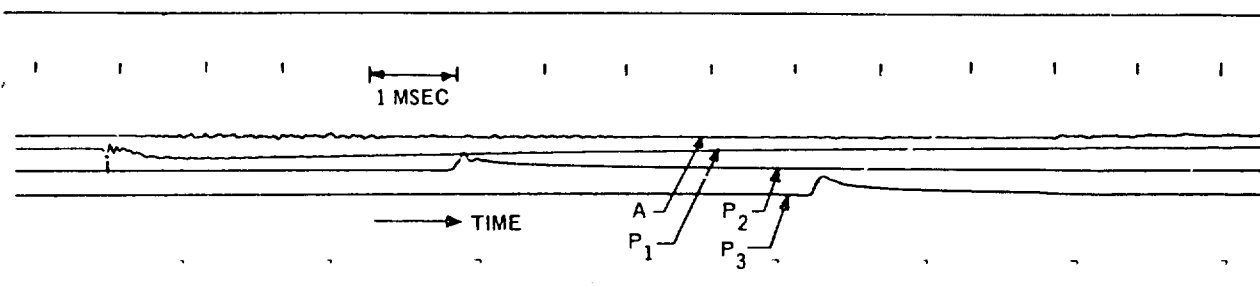


Figure 9c – 6-Degree Deadrise Model

Figure 9 (continued)

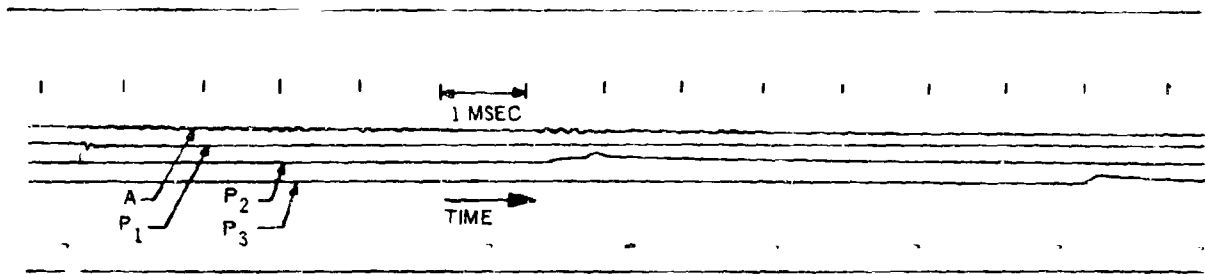


Figure 9d - 10-Degree Deadrise Model

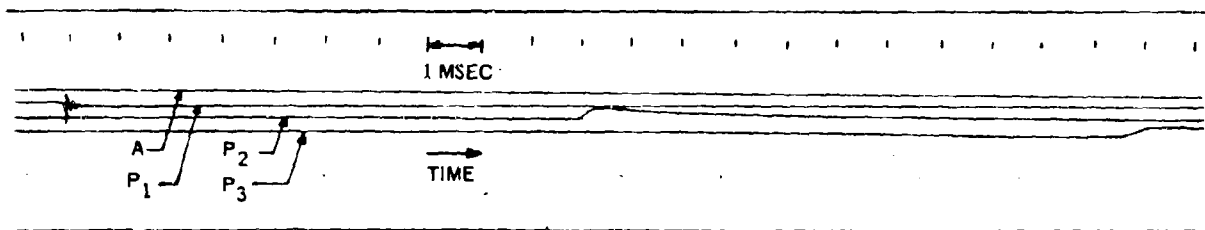


Figure 9e - 15-Degree Deadrise Model

MODEL DEADRISE ANGLE, DEG	1	3	6	10	15
RUN NUMBER	66-78	68-86	66-94	66-99	66-109
DIMENSIONS a - b - c IN.	3 $\frac{29}{32}$ - 7 $\frac{13}{16}$ - 10	3 $\frac{29}{32}$ - 7 $\frac{13}{16}$ - 10	4 - 7 $\frac{29}{32}$ - 9 $\frac{31}{32}$	3 $\frac{7}{8}$ - 7 $\frac{25}{32}$ - 10	3 $\frac{31}{32}$ - 7 $\frac{27}{32}$ - 10 $\frac{1}{32}$
A - ACCELERATION AT KEEL, g	64 MAX.	139 PEAK/PEAK	11 P/P	1.9 P/P	NIL
P - MAXIMUM PRESSURE AT KEEL, PSI (IMPULSE/HYDRO)	0/33	15/11.2	15.3/5.5	28.5/3.8	23.4/2.8
P - MAXIMUM PRESSURE a-IN. OFF KEEL, PSI		46	26.4	12.6	6.8
P - MAXIMUM PRESSURE b-IN. OFF KEEL, PSI	20	48	25	11.8	5.5

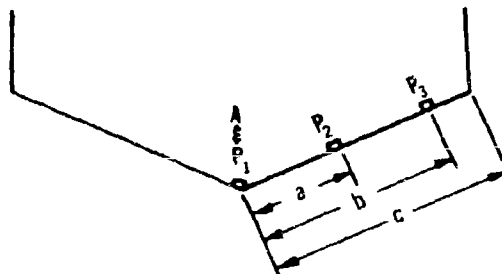


Figure 10 — Experimental Results of Maximum Impact Pressure Due to Rigid Wedge Slamming

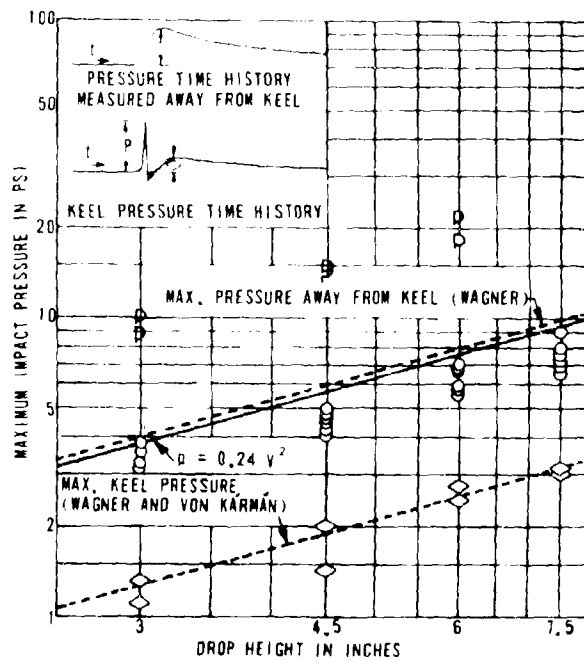


Figure 10a — Model with 15-Degree Deadrise Angle

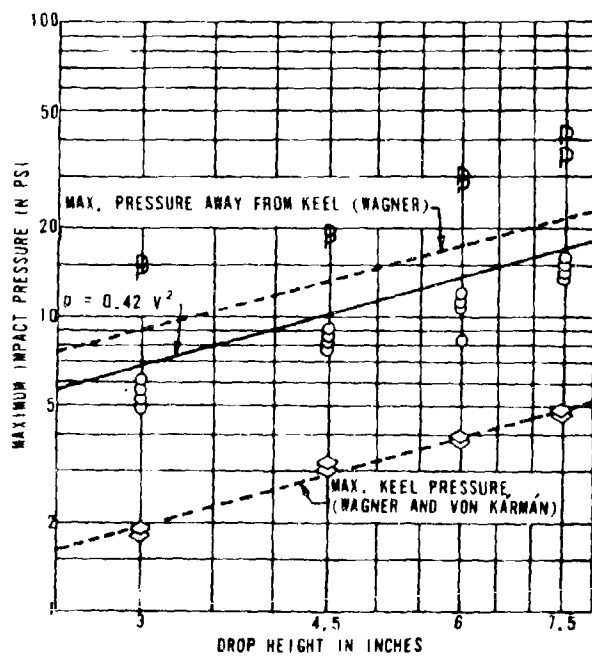


Figure 10b — Model with 10-Degree Deadrise Angle

Figure 10 (continued)

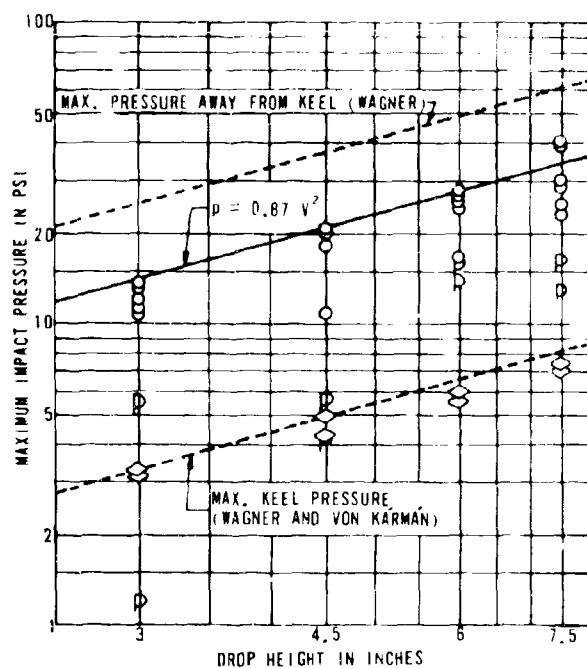


Figure 10c - Model with 6-Degree Deadrise Angle

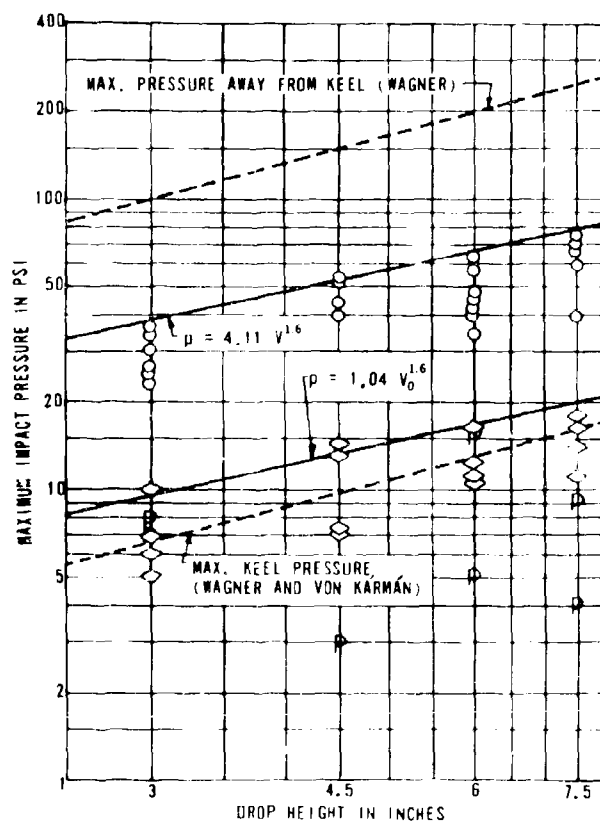


Figure 10d - Model with 3-Degree Deadrise Angle

Figure 10 (continued)

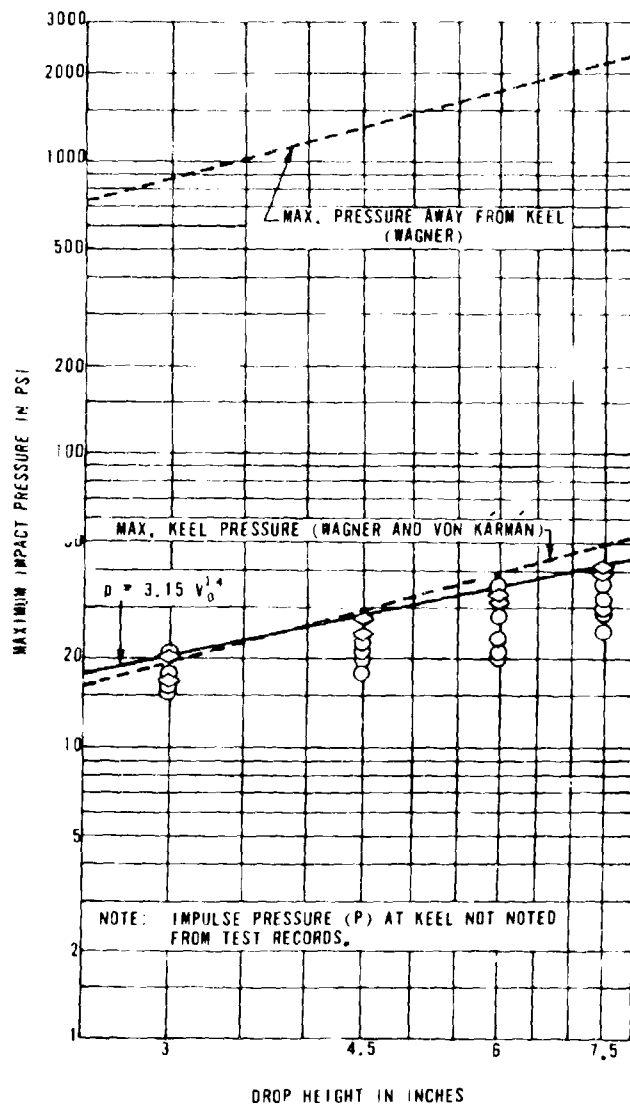


Figure 10e — Model with 1-Degree Deadrise Angle

Figure 11 - Maximum Impact Pressure Due to Rigid Wedge Slamming versus Various Drop Heights

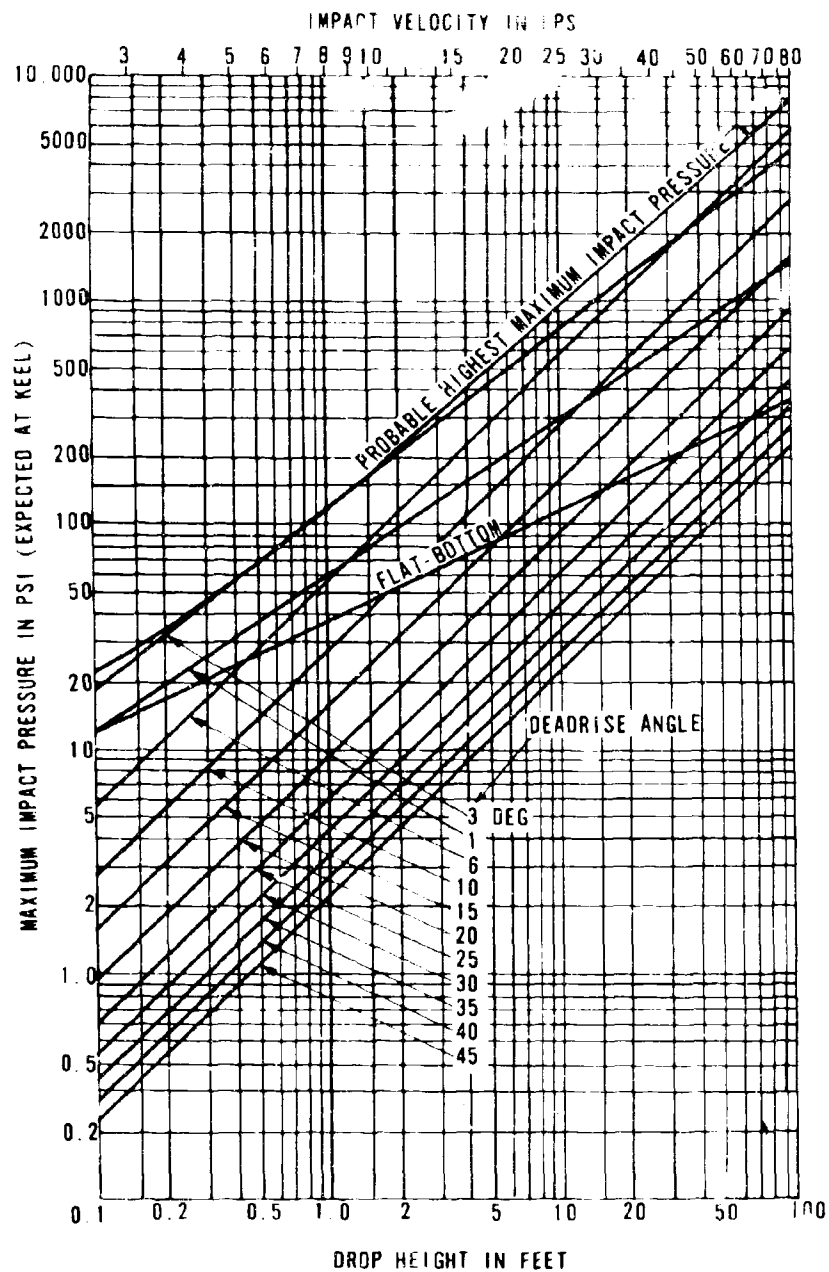


Figure 11a - Pressure away from Keel

Figure 11 (continued)

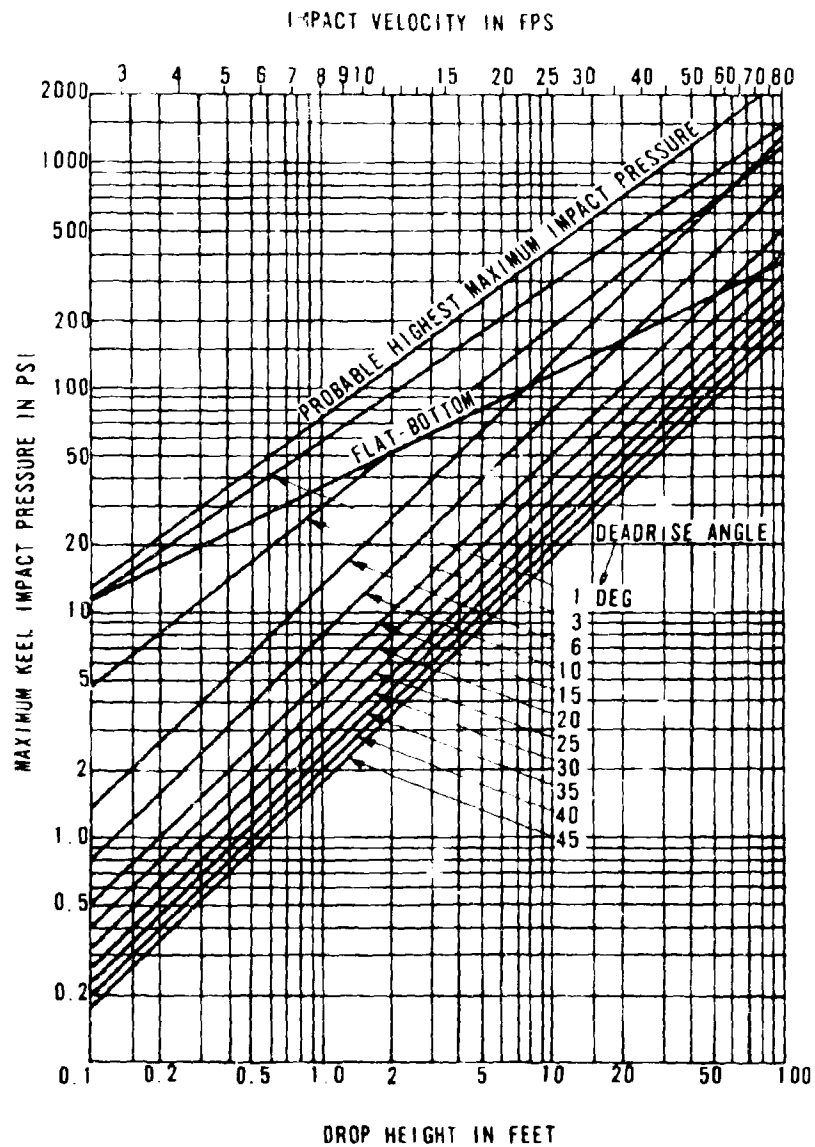


Figure 11b - Keel Pressure

Figure 12 — Maximum Impact Pressure Due to Rigid Wedge Slamming versus Various Deadrise Angles

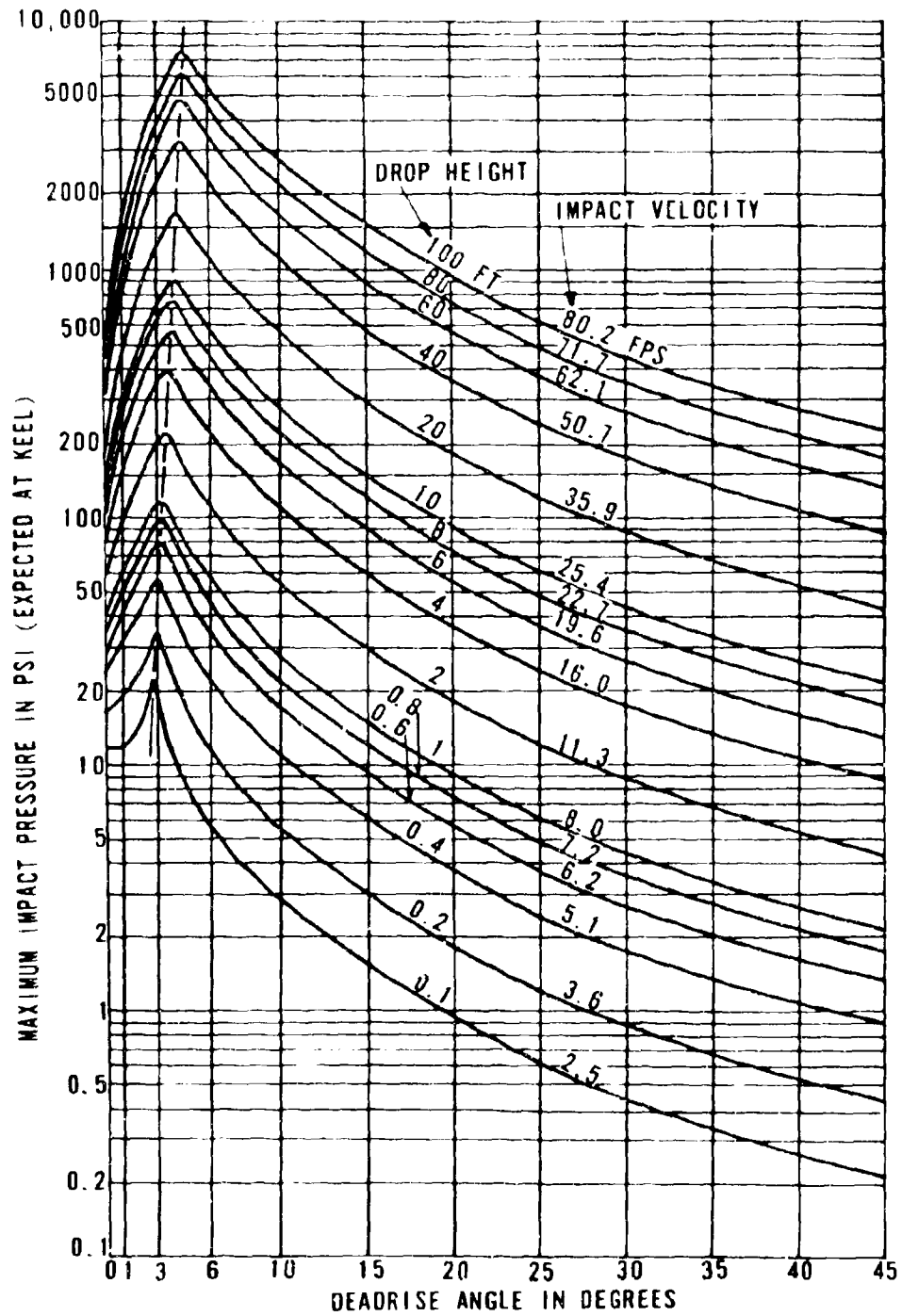


Figure 12a — Pressure away from Keel

Figure 12 (continued)

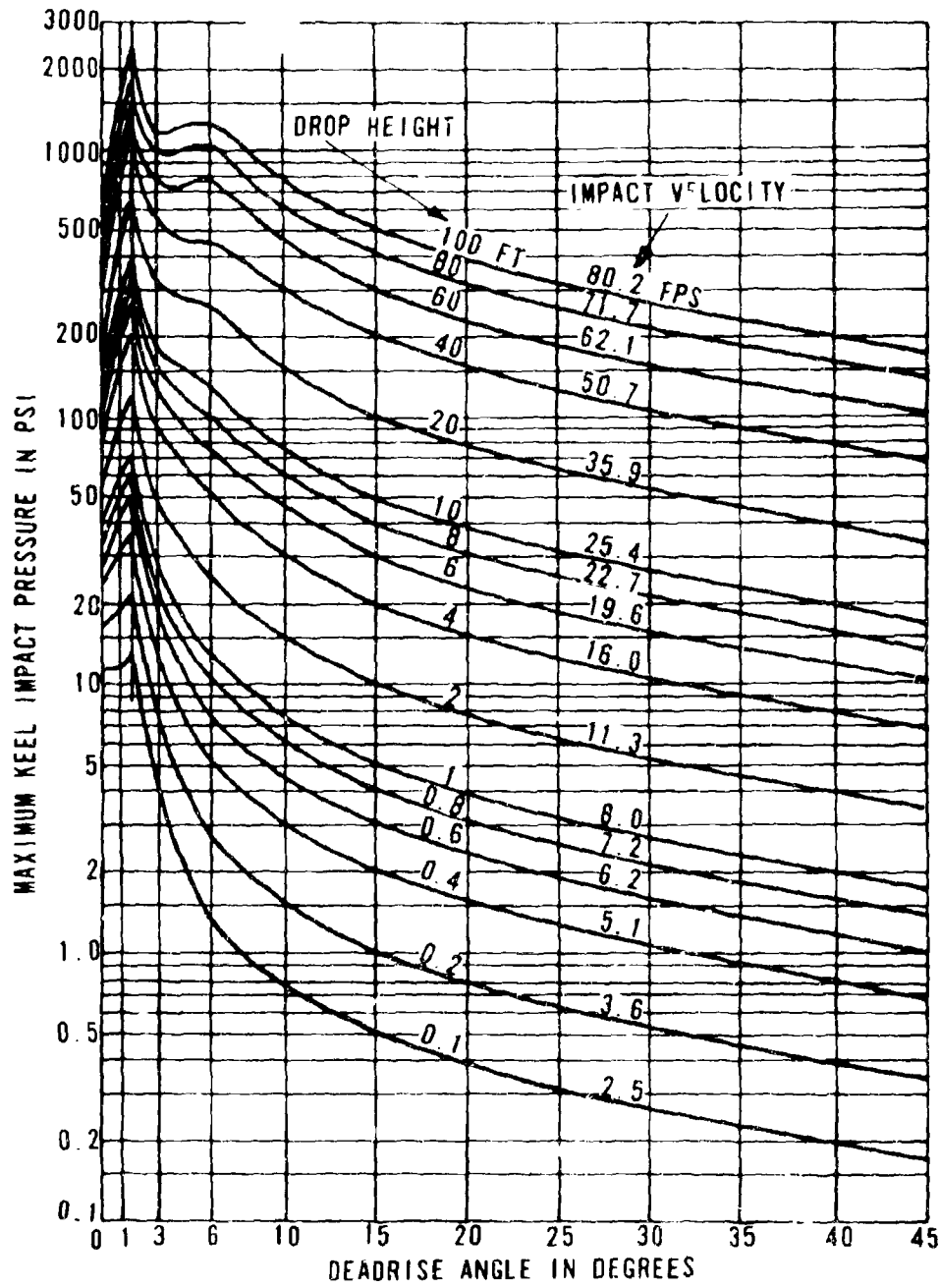


Figure 12b - Pressure at Keel

## REFERENCES

1. Chuang, S.L., "Experimental Investigation of Rigid Flat-Bottom Body Slamming," David Taylor Model Basin Report 2041 (Sep 1965).
2. Chuang, S.L., "Experiments on Flat-Bottom Slamming," Journal of Ship Research, pp. 10-17 (Mar 1966).
3. Vossers, G., Jr., "Resistance, Propulsion and Steering of Ships—Behaviour of Ships in Waves," Technical Publishing Company H. Stam N.V., Haarlem, Netherlands (1962) pp. 189-195, References pp. 203-206.
4. Pierson, J.D., "On the Virtual Mass of Water Associated with an Immersing Wedge," Journal of Aeronautical Sciences (Jun 1951).
5. von Kármán, Th., "The Impact on Seaplane Floats during Landing," National Advisory Committee for Aeronautics TN 321 (1929).

UNCLASSIFIED

Security Classification

## DOCUMENT CONTROL DATA - R&amp;D

(Security classification of title, body of abstract and indexing annotation must be entered when the overall report is classified)

1. ORIGINATING ACTIVITY (Corporate author) Department of the Navy David Taylor Model Basin Washington, D.C. 20007		2a. REPORT SECURITY CLASSIFICATION Unclassified	
		2b. GROUP	
3. REPORT TITLE  SLAMMING OF RIGID WEDGE-SHAPED BODIES WITH VARIOUS LOW DEADRISE ANGLES			
4. DESCRIPTIVE NOTES (Type of report and inclusive dates) Final			
5. AUTHOR(S) (Last name, first name, initial)  Chuang, Sheng-Lun			
6. REPORT DATE October 1966		7a. TOTAL NO. OF PAGES 35	7b. NO. OF REFS 5
8a. CONTRACT OR GRANT NO. Problem No. 765-056		9a. ORIGINATOR'S REPORT NUMBER(S) 2268	
b. PROJECT NO.			
c. Subproject S-R011 01 01		9b. OTHER REPORT NO(S) (Any other numbers that may be assigned this report)	
d. Task 0401			
10. AVAILABILITY/LIMITATION NOTICES  Distribution of this document is unlimited.			
11. SUPPLEMENTARY NOTES		12. SPONSORING MILITARY ACTIVITY Department of the Navy David Taylor Model Basin Washington, D.C. 20007	
13. ABSTRACT  An experimental investigation of rigid body slamming was performed at the David Taylor Model Basin by dropping one flat-bottom steel model and five wedge-shaped steel models with small deadrise angles (from 1 to 15 deg) from various elevated positions above a calm water surface. Recording instrumentation was capable of picking up and recording frequencies from 0 to 200 kc, which covered the frequency range of the hydrodynamic as well as the acoustic pressures that might act on the model. From the test results, a set of charts is provided to predict the maximum impact pressures due to slamming of rigid wedge-shaped bodies.			

DD FORM 1473  
1 JAN 64

UNCLASSIFIED

Security Classification

**UNCLASSIFIED**  
Security Classification

14.	KEY WORDS	LINK A		LINK B		LINK C	
		ROLE	WT	ROLE	WT	ROLE	WT
Flat-Bottom Impact Hydrodynamic Impact Impact of Wedge-Shaped Body Ship Slamming Trapped Air Detection Trapped Air Phenomenon							

**INSTRUCTIONS**

1. **ORIGINATING ACTIVITY:** Enter the name and address of the contractor, subcontractor, grantee, Department of Defense activity or other organization (*corporate author*) issuing the report.
- 2a. **REPORT SECURITY CLASSIFICATION:** Enter the overall security classification of the report. Indicate whether "Restricted Data" is included. Marking is to be in accordance with appropriate security regulations.
- 2b. **GROUP:** Automatic downgrading is specified in DoD Directive 5200.10 and Armed Forces Industrial Manual. Enter the group number. Also, when applicable, show that optional markings have been used for Group 3 and Group 4 as authorized.
3. **REPORT TITLE:** Enter the complete report title in all capital letters. Titles in all cases should be unclassified. If a meaningful title cannot be selected without classification, show title classification in all capitals in parentheses immediately following the title.
4. **DESCRIPTIVE NOTES:** If appropriate, enter the type of report, e.g., interim, progress, summary, annual, or final. Give the inclusive dates when a specific reporting period is covered.
5. **AUTHOR(S):** Enter the name(s) of author(s) as shown on or in the report. Enter last name, first name, middle initial. If military, show rank and branch of service. The name of the principal author is an absolute minimum requirement.
6. **REPORT DATE:** Enter the date of the report as d month, year, or month, year. If more than one date appears on the report, use date of publication.
- 7a. **TOTAL NUMBER OF PAGES:** The total page count should follow normal pagination procedures, i.e., enter the number of pages containing information.
- 7b. **NUMBER OF REFERENCES:** Enter the total number of references cited in the report.
- 8a. **CONTRACT OR GRANT NUMBER:** If appropriate, enter the applicable number of the contract or grant under which the report was written.
- 8b, 8c, & 8d. **PROJECT NUMBER:** Enter the appropriate military department identification, such as project number, subproject number, system numbers, task number, etc.
- 9a. **ORIGINATOR'S REPORT NUMBER(S):** Enter the official report number by which the document will be identified and controlled by the originating activity. This number must be unique to this report.
- 9b. **OTHER REPORT NUMBER(S):** If the report has been assigned any other report numbers (*either by the originator or by the sponsor*), also enter this number(s).
10. **AVAILABILITY/LIMITATION NOTICES:** Enter any limitations on further dissemination of the report, other than those

imposed by security classification, using standard statements such as:

- (1) "Qualified requesters may obtain copies of this report from DDC."
- (2) "Foreign announcement and dissemination of this report by DDC is not authorized."
- (3) "U. S. Government agencies may obtain copies of this report directly from DDC. Other qualified DDC users shall request through \_\_\_\_\_."
- (4) "U. S. military agencies may obtain copies of this report directly from DDC. Other qualified users shall request through \_\_\_\_\_."
- (5) "All distribution of this report is controlled. Qualified DDC users shall request through \_\_\_\_\_."

If the report has been furnished to the Office of Technical Services, Department of Commerce, for sale to the public, indicate this fact and enter the price, if known.

11. **SUPPLEMENTARY NOTES:** Use for additional explanatory notes.

12. **SPONSORING MILITARY ACTIVITY:** Enter the name of the departmental project office or laboratory sponsoring (paying for) the research and development. Include address.

13. **ABSTRACT:** Enter an abstract giving a brief and factual summary of the document indicative of the report, even though it may also appear elsewhere in the body of the technical report. If additional space is required, a continuation sheet shall be attached.

It is highly desirable that the abstract of classified reports be unclassified. Each paragraph of the abstract shall end with an indication of the military security classification of the information in the paragraph, represented as (TS), (S), (C), or (U).

There is no limitation on the length of the abstract. However, the suggested length is from 150 to 225 words.

14. **KEY WORDS:** Key words are technically meaningful terms or short phrases that characterize a report and may be used as index entries for cataloging the report. Key words must be selected so that no security classification is required. Identifiers, such as equipment model designation, trade name, military project code name, geographic location, may be used as key words but will be followed by an indication of technical context. The assignment of links, rules, and weights is optional.

**UNCLASSIFIED**

Security Classification